MOLECULAR AND CELLULAR BIOLOGY, June 2005, p. 4565–4578 Vol. 25, No. 11
0270-7306/05/$08.00+0 doi:10.1128/MCB.25.11.4565–4578.2005

Decreased Growth of *Vhl*$^{-/-}$ Fibrosarcomas Is Associated with Elevated Levels of Cyclin Kinase Inhibitors p21 and p27

Fiona A. Mack,[1,2] Jagruti H. Patel,[2] Mangatt P. Biju,[3] Volker H. Haase,[2,3] and M. Celeste Simon[1,2,4]*

Abramson Family Cancer Research Institute,[1] Cell Growth and Cancer Graduate Group,[2] Department of Medicine,[3] and Howard Hughes Medical Institute,[4] University of Pennsylvania, Philadelphia, Pennsylvania 19104

Received 28 September 2004/Returned for modification 8 November 2004/Accepted 25 February 2005

Inactivating mutations within the von Hippel-Lindau (*VHL*) tumor suppressor gene predispose patients to develop a variety of highly vascularized tumors. pVHL targets α subunits of the heterodimeric transcription factor hypoxia-inducible factor (HIF), a critical regulator of energy metabolism, angiogenesis, hematopoiesis, and oxygen (O_2) delivery, for ubiquitin-mediated degradation in an O_2-dependent manner. To investigate the role of *Vhl* in cellular proliferation and tumorigenesis, we utilized mouse embryonic fibroblasts (MEFs), a common tool for analyzing cell cycle regulation, and generated *Vhl*$^{-/-}$ MEF-derived fibrosarcomas. Surprisingly, growth of both *Vhl*$^{-/-}$ MEFs and fibrosarcomas was impaired, although tumor vascularity was increased. Decreased proliferation of *Vhl*$^{-/-}$ MEFs was correlated with an overexpression of cyclin kinase inhibitors (CKIs) p21 and p27. The transcription of p21 and p27 is inhibited by c-Myc; therefore, the induction of CKIs was attributed to the ability of HIF to antagonize c-Myc activity. Indeed, p21 mRNA levels were elevated under normoxia in *Vhl*$^{-/-}$ MEFs, while c-Myc transcriptional activity was markedly reduced. Gene silencing of HIF-1α by small interfering RNA reduced p21 and p27 protein and mRNA levels in *Vhl*$^{-/-}$ MEFs. The induction of p21 and p27, mediated by constitutive activation of the HIF pathway, provides a mechanism for the decreased proliferation rates of *Vhl*$^{-/-}$ MEFs and fibrosarcomas. These results demonstrate that a loss of pVHL can induce growth arrest in certain cells types, which suggests that additional genetic mutations are necessary for *VHL*-associated tumorigenesis.

von Hippel-Lindau disease is a hereditary cancer syndrome in which inheritance of an inactivating mutation within the von Hippel-Lindau (*VHL*) gene predisposes patients to the development of pheochromocytomas, renal clear-cell carcinomas, and hemangiomas affecting the central nervous system and retina (27). *VHL*-mediated disease conforms to the Knudson "two-hit" hypothesis for a tumor suppressor; complete loss of gene activity is achieved by a second inactivating mutation within somatic cells. In agreement with this hypothesis, a majority of sporadic renal clear-cell carcinomas exhibit biallelic loss of *VHL* (7).

Insight into the role of pVHL as a tumor suppressor can be found in its ability to form an E3 ubiquitin ligase complex that binds and degrades the hypoxia-inducible factor (HIF) α subunits (32). HIF, a heterodimeric transcription factor, is the primary regulator of both cellular and systemic responses to decreased O_2 concentrations which include enhanced glycolysis, angiogenesis, and erythropoiesis. Under normoxic or atmospheric O_2 levels (21%), hydroxylation of key proline residues within regulatory oxygen-dependent degradation domains (ODDs) of HIF-α subunits facilitates pVHL binding (17, 18, 41). Under limiting O_2 conditions, proline hydroxylation is inhibited, thereby stabilizing HIF-α subunits which then translocate into the nucleus and bind to constitutively stabilized HIF-β subunits. HIF activates such O_2-responsive genes as glucose transporter 1 (*GLUT-1*), aldolase A (*ALDA-A*), phosphoglycerate kinase (*PGK*), vascular endothelial growth factor (*VEGF*), and erythropoietin (*EPO*). Loss of pVHL therefore leads to the activation of HIF and HIF target genes, mimicking a constant hypoxic state under normoxic conditions. Indeed, *VHL*$^{-/-}$ renal clear-cell carcinomas and embryonic stem (ES) cells exhibit constitutive HIF-α stabilization and activation of hypoxia-induced genes, while reintroduction of pVHL into *VHL*$^{-/-}$ cell lines restores HIF regulation (25, 26, 32).

The development of renal clear-cell carcinomas may be dependent upon additional cellular pathways that are disrupted in the absence of pVHL. Recent studies have shown that pVHL binds other proteins and affects a variety of cellular processes, suggesting multiple functions for pVHL beyond the regulation of HIF. Consistent with their tumorigenic phenotype, *VHL*$^{-/-}$ renal clear-cell carcinoma cell lines (RCCs) display several defects in cell cycle regulation. Upon serum withdrawal, *VHL*$^{-/-}$ RCCs fail to exit the cell cycle due to a lack of p27 accumulation (36). Furthermore, cyclin D1 levels are elevated within *VHL*$^{-/-}$ RCCs and remain high under conditions that promote contact inhibition (2, 4). Cyclin D1 has been suggested to be an HIF target gene in *VHL*$^{-/-}$ kidney cells, contributing to their unregulated cell growth (40). pVHL also seems to affect extracellular matrix (ECM) assembly via fibronectin deposition, actin and vinculin localization to focal adhesions, microtubule stabilization, and ubiquitination of protein kinase C isoforms; however, the contribution of these pathways to VHL disease has not been thoroughly examined (14, 20, 33, 34). A majority of these effects are independent of pVHL's function in an E3 ubiquitin ligase complex and may

* Corresponding author. Mailing address: University of Pennsylvania School of Medicine, Abramson Family Cancer Research Institute, Howard Hughes Medical Institute, Rm. 438 BRBII/III, 421 Curie Blvd., Philadelphia, PA 19104. Phone: (215) 746-5561. Fax: (215) 746-5511. E-mail: celeste2@mail.med.upenn.edu.

therefore be a secondary effect of tumor progression, highlighting the potential complexity of isolating the role of pVHL in tumorigenesis in established cancer cell lines.

Although the loss of pVHL affects a variety of cellular processes, dysregulation of HIF appears to be essential for renal tumorigenesis. Overexpression of a peptide derived from the ODD of HIF-1α in $VHL^{+/+}$ RCCs restores the ability of these cells to form tumors in nude mice but does not fully recapitulate the clear-cell phenotype (31). RCCs infected with a retrovirus producing constitutively stabilized HIF-2α generate rapidly growing subcutaneous tumors that appear more malignant than controls (22). Conversely, depletion of HIF-2α by the use of short hairpin RNAs inhibits tumor formation and abrogates hypoxic gene responses (21, 42). In addition, HIF activation can be detected within early kidney lesions of *VHL* patients and correlates with biallelic loss of *VHL* (30). These results suggest that HIF-α stabilization and activation are a critical downstream target in *VHL*-induced renal tumorigenesis.

Whereas hypoxia-induced pathways of angiogenesis are necessary for solid tumor growth, no tumors to date have been found to harbor direct mutations in HIF leading to its dysregulation. Indeed, hypoxia decreases cellular proliferation in a variety of cell types. Very low O_2 tensions (0.01%) lead to inhibition of DNA replication and S-phase arrest; reentry into the cell cycle upon reoxygenation is regulated by the activity of the cyclin kinase inhibitors (CKIs) p21 and p27 (12). More moderate levels of hypoxia (0.1 to 0.5% O_2) also inhibit G_1/S transition through the induction of p27 and hypophosphorylation of pRB (8). Hypoxia-induced growth arrest has been demonstrated in primary cells such as mouse embryonic fibroblasts (MEFs) and B cells (11). Hypoxic induction of p21 and p27 was initially reported to be HIF independent due to a lack of a hypoxia-responsive element (HRE) within their promoter regions. Recent work has suggested a novel mechanism by which HIF can induce p21 and p27 levels by antagonizing c-Myc transcriptional activity. HIF can bind and displace c-Myc from the proximal promoter region of c-Myc responsive genes, thereby relieving c-Myc repression of p21 and p27 (23). These results provide an explanation for the hypoxic induction of p21 and p27 in the absence of HREs within their promoter regions.

The effects of hypoxia on cell cycle progression appear inconsistent with the observed cell cycle defects of $VHL^{-/-}$ RCCs. Subcutaneous tumors derived from $VHL^{-/-}$ RCCs grow rapidly and overexpress cyclin D1 (9, 16), although the HIF pathway is dysregulated. To further examine the effects of pVHL loss and constitutive HIF activation on cell cycle progression and growth of solid tumor, we employed MEFs with a conditionally targeted *Vhl* allele. MEFs are a common tool used to study cell cycle regulation and have the advantage of harboring defined genetic alterations as opposed to the highly aneuploid RCCs. Fibrosarcomas were generated by injecting immortalized, transformed MEFs subcutaneously into immunocompromised mice. Surprisingly, $Vhl^{-/-}$ fibrosarcomas were significantly smaller than control tumors. The growth defect of $Vhl^{-/-}$ fibrosarcomas resulted from a substantial decrease in cellular proliferation as opposed to an increase in apoptosis. In vitro analysis of $Vhl^{-/-}$ MEFs revealed an increase in p21 and p27 protein levels which correlated with a decrease in cellular proliferation. Genetic silencing of HIF-1α and c-Myc by small interfering RNA (siRNA) in $Vhl^{-/-}$ MEFs revealed that the elevated levels of p21 and p27 result from constitutive HIF activity and antagonism of c-Myc-mediated repression of these CKIs. We suggest that pVHL loss can be detrimental to specific cell types through the induction of HIF-mediated growth arrest. These results substantiate the hypothesis that additional mutations must occur to fully promote *VHL* tumorigenesis and provide insight into the tissue specificity of VHL disease.

MATERIALS AND METHODS

Isolation of $Vhl^{+/+}$ and $Vhl^{-/-}$ MEFs. Embryos carrying the 2-lox alleles for *Vhl* were harvested at embryonic day 13.5 (E13.5) and dissociated by incubation in 0.5% trypsin–EDTA. Cells were immortalized by stable transfection with simian virus 40 large T antigen (Ag) by using FUGENE (Roche) according to the manufacturer's instructions and transformed with a retrovirus expressing H-Ras (19). Immortalized, transformed MEFs were infected with a control adenovirus expressing either β-galactoside or green fluorescent protein (GFP) or an adenovirus expressing Cre recombinase or Cre recombinase conjugated with GFP. GFP-expressing adenoviruses were obtained from the Baylor College of Medicine Vector Development Laboratory.

Western blot analysis. For all Western blot assays, cells were plated such that the density of the cells at the time of lysis was ~60 to 70% confluent. Hypoxia, defined as 1.5% or 0.5% O_2 where indicated, was generated using an In Vivo$_2$ hypoxic workstation (Ruskinn Technologies, Leeds, United Kingdom) or an IG750 variable O_2 tissue culture incubator (Jouan Inc.). Biocoat fibronectin-coated and poly-L-lysine plates were purchased from Becton Dickinson.

Whole-cell protein lysates were prepared using WCE buffer (150 mM NaCl, 50 mM Tris, pH 7.4, 5 mM EDTA, 0.1% sodium dodecyl sulfate, and Complete protease inhibitor [Roche Molecular Biochemicals]) or immunoprecipitation buffer (50 mM HEPES, pH 8.0, 150 mM NaCl, 2.5 mM EGTA, 1 mM EDTA, 0.1% Tween 20, and protease inhibitors). Nuclear and cytoplasmic fractions of protein extracts were prepared using a modified Dignam protocol (28), with buffer A further modified to contain 0.1% NP-40 and buffer C containing 300 mM NaCl. For hypoxic extracts, cells were manipulated inside a hypoxic chamber using phosphate-buffered saline and buffer A that had been equilibrated to the hypoxic environment. Extracts were electrophoresed, transferred, and immunoblotted according to standard protocols using 5% nonfat dry milk (Carnation) in Tris-buffered saline-Tween 20 as a blocking agent. Blots were stained with Ponceau S to ensure equal loading. Antibodies used included anti-mouse pVHL, anti-p21, and anti-c-Myc (Santa Cruz); anti-human pVHL (Pharmingen); anti-mouse HIF-1α and HIF-2α (Novus); anti-mouse HIF-1α (Cayman); anti-AKT, anti-activated caspase-3, anti-P-CDK2 (Cell Signaling Technologies); anti-cyclin D (NeoMarker); anti-p27 (BD Pharmingen); and anti-CDK2 (BD Transduction). Horseradish peroxidase-conjugated anti-rabbit and anti-mouse secondary antibodies were purchased from Cell Signaling Technologies and used at dilutions of 1:2,000. Enhanced chemiluminescence reagents were purchased from Amersham Biosciences. Blots were stripped in 61.5 mM Tris (pH 6.8), 2% sodium dodecyl sulfate, and 100 mM β-mercaptoethanol at 55°C for 1 h before being blocked and reprobed.

Northern analysis. For Northern blots, 2×10^6 to 3×10^6 cells/10-cm tissue culture dish were plated and allowed to recover overnight. Where indicated, cells were incubated in hypoxia for 18 h. All cells were lysed in Trizol (Invitrogen) according to the manufacturer's instructions in ambient air. Twenty micrograms of total RNA was electrophoresed in 1.5% denaturing (formaldehyde) agarose gels and transferred to Hybond N^+ membranes (Amersham). Murine *Pgk*, *Alda*, and *Glut-1* probes have been previously described (29).

VEGF enzyme-linked immunosorbent assay. VEGF quantitation was performed using the Quantikine M murine immunoassay kit, (R&D Systems) according to the manufacturer's protocol. A total of 7.5×10^5 cells were seeded onto 12-well plates and incubated in hypoxia for 18 h where indicated. Conditioned medium was incubated with a mouse-specific VEGF polyclonal antibody bound to a microtiter plate. After several washes, a second enzyme-linked polyclonal antibody specific for mouse VEGF was added. Sample values were obtained according to the manufacturer's protocol. Recorded values were normalized for cell number.

Mouse fibrosarocoma assays. A total of 0.5×10^7 to 1×10^7 cells were suspended in 100 μl of phosphate-buffered saline (Gibco) and injected subcutaneously into the dorsal area of 4- to 6-week-old female NIH-III immunodeficient mice (Taconic). After 7 days, tumors were measured every 2 to 3 days with calipers in the two greatest dimensions to calculate tumor volume. After 12 to 14

days, fibrosarcomas were excised, photographed, weighed, frozen for protein assays, and fixed in 4% paraformaldehyde.

Immunohistochemistry. Tumor samples were fixed in 4% paraformaldehyde and paraffin embedded by standard techniques. Sections (6 μm) of each sample were incubated overnight with antibodies generated against cleaved caspase-3 (Cell Signaling Technologies), Ki67 (Novacastra), bromodeoxyuridine (BrdU) (BD-Pharmigen), and CD34 (BD Scientific). A terminal deoxynucleotidyltransferase-mediated dUTP-biotin nick end labeling (TUNEL) assay, the *In Situ* Cell Death Detection kit, was utilized according to the manufacturer's protocol (Roche). Anti-mouse and anti-rat secondary antibodies were biotinylated, and staining was achieved by a streptavidin-biotin system conjugated with horseradish peroxidase (Vector Laboratories). CD34, Ki67, BrdU, and cleaved caspase-3 photographs were taken with a Leica DC500 camera. Morphometric analysis was performed on three to five randomly chosen sections of each tumor using the analytical program Image Pro (Phase 3 Imaging). The number of positive cells was calculated as the total area of positive staining divided by the area of an individual positive cell. The percentage of positive cells was calculated as the number of positive cells divided by the total number of cells.

Tomato lectin perfusion. One hundred microliters of Flourescein-Lycopersicon esculentum (tomato) lectin (Vector Labs) was injected into mouse tail veins at a dose of 2 mg/ml. Tumors were internally fixed with 4% paraformaldehyde and paraffin embedded. Sections of 15 to 20 μm were used for confocal analysis.

BrdU labeling. For fibrosarcomas, 50 μl of BrdU (10 mg/ml) (Sigma) was injected intraperitoneally 2 hours prior to tumor dissection. Tumors and sections were processed according to general immunohistochemistry protocols. Monolayer cultures of MEFs were pulsed for 30 min with 3 μg/ml of BrdU. Cells were fixed with 70% ethyl alcohol. Incubation with anti-BrdU antibody was performed according to the manufacturer's protocol (BD-Pharmigen).

In vitro kinase assay. MEFs were lysed in 1 ml of 0.1% NP-40 lysis buffer containing 50 mM HEPES (pH 7.8), 250 mM NaCl, 1 mM EGTA, 1 mM dithiothreitol, and 10% glycerol with protease and phosphatase inhibitors. Three hundred micrograms of cellular lysate was utilized for the kinase assay. The samples were precleared with protein A/G agarose (Pierce) and were incubated with anti-cyclin E (Santa Cruz), anti-cyclin A (Santa Cruz), anti-CDK2 (BD Transduction), or anti-CDK4 (Upstate) at 4°C for 1 h. Protein A/G agarose was added to the lysate, and the mixture was incubated overnight at 4°C. After three washes with lysis buffer and three washes with kinase reaction buffer (50 mM HEPES [pH 7.4], 1 mM dithiothreitol, 10 mM $MgCl_2$), the beads were resuspended in 30 μl of buffer containing 1 μg of histone H1 (Roche) or 1 μg of retinoblastoma protein (RB) (Upstate), 20 μM ATP, and 10 μCi of [γ^{32}P]ATP (Amersham). The reaction was terminated after a 30-min incubation at 30°C by adding 6 μl of 5× loading dye. Samples were run on sodium dodecyl sulfate–15% polyacrylamide gels and transferred into nitrocellulose for immunoblotting.

Real-time PCR. Total RNA was purified from cells using Trizol reagent (Life Technologies). Mixed oligo$(dT)_{15}$ and ribosomal 18S RNA-specific primers were used to generate single-stranded cDNAs, which were assayed for levels of *Vegf-A*, phosphoglycerate kinase (*Pgk*), c-*Myc*, *p21*, *p27*, and 18S transcripts using an Applied Biosystems 7900HT sequence detection system. Mixed primer/probe sets for each transcript were obtained from Applied Biosystems and used according to the manufacturer's instructions. Expression levels of *Vegf*, *Pgk*, c-*Myc*, *p21*, and *p27* transcripts were normalized to endogenous ribosomal 18S transcripts. Data comparisons were made by $\Delta\Delta C_T$ comparative analysis using the manufacturer's software.

Reporter assays. The HRE-luciferase reporter constructs were previously described (1). Transfection efficiency was assessed by cotransfection of a *Renilla* luciferase gene under the control of a minimal tyrosine kinase promoter. Where indicated, cells were also cotransfected with a plasmid encoding hemagglutinin-tagged full-length human pVHL. The c-Myc reporter construct was a kind gift of Jay Hess, and a c-Myc expression plasmid was a gift of Thomas Yang. For transient transfections, 1×10^6 MEFs were plated onto 6-well plates and allowed to recover overnight. Cells were transfected the next morning using Lipofectamine Plus reagent (Gibco BRL) according to the manufacturer's protocol. Cells were transfected for 4 h, and one-half of each sample was exposed to hypoxia for 36 h. Proteins were extracted from samples using reporter lysis buffer, and dual luciferase assays were performed according to the manufacturer's guidelines (Promega).

siRNA transfection. Gene silencing was achieved by transient transfection of siRNA oligonucleotides purchased from Dharmacon according to the manufacturer's protocol. In brief, MEFs were plated overnight in antibiotic-free medium to reach 50% confluency. Cells were transfected the following morning using Lipofectamine 2000 (Gibco BRL) with 100 pmol/ml of siRNA oligonucleotides as described above. After exposure to 0.5% O_2 for 48 h, cells were harvested for protein and RNA.

RESULTS

Generation of immortalized and transformed *Vhl*$^{-/-}$ MEFs. Due to the fact that the loss of pVHL results in lethality at E9.5 (10), MEFs were generated from E13.5 mouse embryos homozygous for a previously described conditional *Vhl* allele (13) (Fig. 1). In order to establish a continuously growing cell line to analyze the role of pVHL in cellular proliferation and tumor growth, *Vhl*$^{+/+}$ MEFs containing the 2-lox allele were immortalized with simian virus 40 large T antigen and transformed with an activating mutation in H-Ras. Immortalized, transformed *Vhl*$^{+/+}$ cells were infected with either an adenovirus expressing Cre recombinase to generate MEFs homozygous for a mutant *Vhl* allele or a control adenovirus expressing β-galactosidase. Cre recombinase expression resulted in gene excision in greater than 90% of expressing cells. PCR analysis revealed the exclusive presence of the recombined allele in *Vhl*$^{-/-}$ MEFs after infection with the Cre-expressing adenovirus (Fig. 1B). Furthermore, two pVHL isoforms (a 19-kDa species and a smaller polypeptide) expressed in MEFs were undetectable in *Vhl*$^{-/-}$ extracts (Fig. 1C). To ensure a homogeneous culture for in vitro assays, *Vhl*$^{+/+}$ MEFs were also infected with an adenovirus expressing Cre recombinase conjugated with GFP or a control adenovirus expressing GFP alone and sorted by a fluorescence-activated cell sorter for GFP expression (data not shown). Subsequent *Vhl*$^{-/-}$ MEFs were characterized for dysregulation of the HIF pathway, in terms of protein stabilization, nuclear translocation, and activation of downstream target genes.

Constitutive HIF stabilization and target gene activation in *Vhl*$^{-/-}$ MEFs. HIF-1α protein levels were stabilized under hypoxia in *Vhl*$^{+/+}$ MEFs and detected only within nuclear fractions of protein extracts. In direct contrast, HIF-1α protein was stabilized under normoxic conditions in *Vhl*$^{-/-}$ MEFs and not further increased upon exposure to 1.5% O_2 (Fig. 1D). Irrespective of the presence of pVHL, HIF-2α protein levels were undetectable in immortalized, transformed MEFs (data not shown). mRNA analysis of HIF target genes revealed an approximate twofold hypoxic induction of *Glut-1*, *Alda-A*, and *Pgk* in *Vhl*$^{+/+}$ MEFs compared to that of normoxia. Consistent with pVHL's role in the regulation of HIF activation, *Vhl*$^{-/-}$ MEFs exhibited elevated levels of HIF target genes under normoxia which were not further induced by hypoxia (Fig. 1E). Additionally, secretion of the HIF target VEGF was elevated in the absence of pVHL under normoxic conditions and not further induced by culture at 1.5% O_2 (Fig. 1F). The expression of pVHL in MEFs is therefore essential for the regulation of HIF-1α protein stability and transactivation of HIF downstream target genes.

***Vhl*$^{-/-}$ fibrosarcomas are significantly smaller than controls.** The development of renal clear-cell carcinomas, pheochromocytomas, and hemangioblastomas is associated with a loss of pVHL. Injection of RCCs into nude mice produces rapidly growing, highly vascularized tumors, consistent with the human disease (9, 15, 16). Nevertheless, teratomas formed from *Vhl*$^{-/-}$ ES cells are significantly smaller than controls, although they are highly vascularized (26). Distinguishing between effects on cellular differentiation and/or proliferation is difficult within teratoma tumor models: the tumor cell population is inherently heterogeneous due to the ability of ES cells

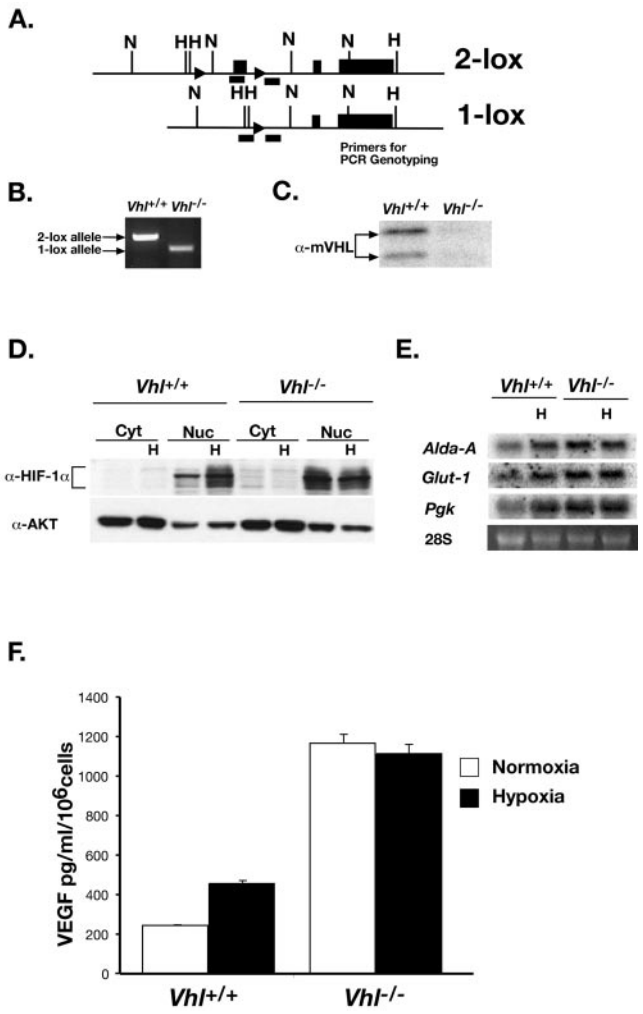

FIG. 1. HIF stabilization and activation of target genes in $Vhl^{+/+}$ and $Vhl^{-/-}$ MEFs. (A) Schematic of genomic *Vhl* 2-lox allele and 1-lox allele after Cre recombination. Exons 1 to 3 are represented by black boxes. Abbreviations for restriction sites: H, HindIII; N, NcoI. (B) PCR genotyping of MEFs after Cre recombination. Only the 1-lox allele was apparent in cells that express Cre recombinase. (C) Western blot for pVHL indicates that the isoforms of 19 kDa and lower are predominant in MEFs. No pVHL was detected in $Vhl^{-/-}$ cells that harbor the 1-lox allele. (D) Immunoblot assay for HIF-1α, after 1.5% O_2 exposure for 4 h, in cytoplasmic and nuclear fractions revealed that stabilized HIF-1α accumulated solely in the nucleus of $Vhl^{-/-}$ MEFs. Akt protein levels, although more abundant in cytoplasmic fractions, demonstrated that equivalent protein amounts were loaded per cell sample. (E) Total RNA isolated from $Vhl^{+/+}$ and $Vhl^{-/-}$ MEFs was probed for *Glut-1*, *Pgk*, and *Alda-A*. Expression of HIF target genes was abundant under normoxia and failed to be further induced by hypoxia in $Vhl^{-/-}$ MEFs. Ethidium bromide staining of 18S RNA was used to indicate equivalent loading. (F) In vitro secretion of VEGF was measured by enzyme-linked immunosorbent assay. VEGF secretion was induced by hypoxia in $Vhl^{+/+}$ MEFs, while levels remained largely unchanged in $Vhl^{-/-}$ MEFs.

to differentiate into cells lines representative of all three germ layers. Therefore, the function of pVHL in cellular proliferation and tumor formation was examined in terminally differentiated MEFs. Wild-type and *Vhl* mutant MEFs were injected subcutaneously into immunocompromised mice. Tumor growth was assessed by volume measurements, and tumor mass was determined upon excision at 12 to 14 days postinjection. Similar to the results obtained with $Vhl^{-/-}$ teratomas, $Vhl^{-/-}$ fibrosarcomas grew significantly slower than controls, as measured by tumor volume, and exhibited a 45% reduction in mass compared to that of controls (Fig. 2B and C). No overt differences in fibrosarcoma histology were evident between genotypes as determined by hematoxylin and eosin staining (Fig. 3A). Furthermore, gross morphology and hematoxylin and eosin staining of fibrosarcomas did not reveal any hemorrhagic regions present within either $Vhl^{+/+}$ or $Vhl^{-/-}$ tumors (Fig. 2A and 3A and B). These results confirm that the loss of pVHL is not essential for solid tumor growth within teratoma and fibrosarcoma tumor models.

Enhanced vascular permeability and density in $Vhl^{-/-}$ fibrosarcomas. Subcutaneous tumor models can exaggerate antitumorigenic effects due to the inherent avascularity of the microenvironment (5). One possible explanation for the decreased growth of $Vhl^{-/-}$ fibrosarcomas is a reduction in tumor vasculature. Therefore, tumor vessel density and permeability were assessed by two methods to demarcate endothelial cells, tomato lectin perfusion and CD34 staining. Confocal analysis of lectin-perfused wild-type tumor sections revealed highly organized vessels with a defined branching pattern and little background lectin staining (Fig. 3C). In contrast, $Vhl^{-/-}$ tumor vessels were smaller, were greatly disorganized, and lacked extensive branching. Furthermore, vascular permeability was increased in $Vhl^{-/-}$ fibrosarcomas, as evidenced by the increase in background lectin staining resulting from the leakage of perfused lectin from blood vessels (Fig. 3D). Vessels visualized by anti-CD34 staining complemented the lectin perfusion images for $Vhl^{+/+}$ fibrosarcomas (Fig. 3E). Detection of microvessels was enhanced by CD34 staining of $Vhl^{-/-}$ fibrosarcomas, revealing a significant increase in mean vessel density compared to that of the control (Fig. 3F). The increase in mean vessel density and vascular permeability was consistent with the elevated expression of angiogenic factors in $Vhl^{-/-}$ MEFs, i.e., VEGF (Fig. 1F). Vascularization is essential to the growth of subcutaneous tumors; however, $Vhl^{-/-}$ fibrosarcomas and $Vhl^{-/-}$ teratomas represent particular situations in which a discontinuity exists between tumor growth and vasculature. These results imply that cellular proliferation and/or apoptotic defects exist that negatively affect $Vhl^{-/-}$ tumor growth.

Growth defect of $Vhl^{-/-}$ fibrosarcomas results from decreased proliferation and not an increase in apoptosis. The large array of HIF target genes includes proapoptotic and, paradoxically, both positive and negative regulators of cellular proliferation (6, 11, 39, 40). The growth defects of *Vhl*-null tumors may in turn be a result of HIF-mediated effects on proliferation and/or apoptosis. Tumor cell proliferation was determined by measuring BrdU incorporation into cells progressing through S phase and immunostaining for the proliferation marker Ki67, which is expressed in all cells not in G_0. The number of cells in S phase and the number of actively cycling cells in $Vhl^{-/-}$ tumors were significantly reduced compared to $Vhl^{+/+}$ fibrosarcomas (Fig. 4A to D). Morphometric analysis demonstrated a 40% reduction in the number of $BrdU^+$ cells in $Vhl^{-/-}$ tumors compared to the wild type (Fig. 4I). Within $Vhl^{-/-}$ tumors, 42% of the cells were $Ki67^+$, compared to 55% $Ki67^+$ cells in $Vhl^{+/+}$ tumors (Fig. 4J). A greater

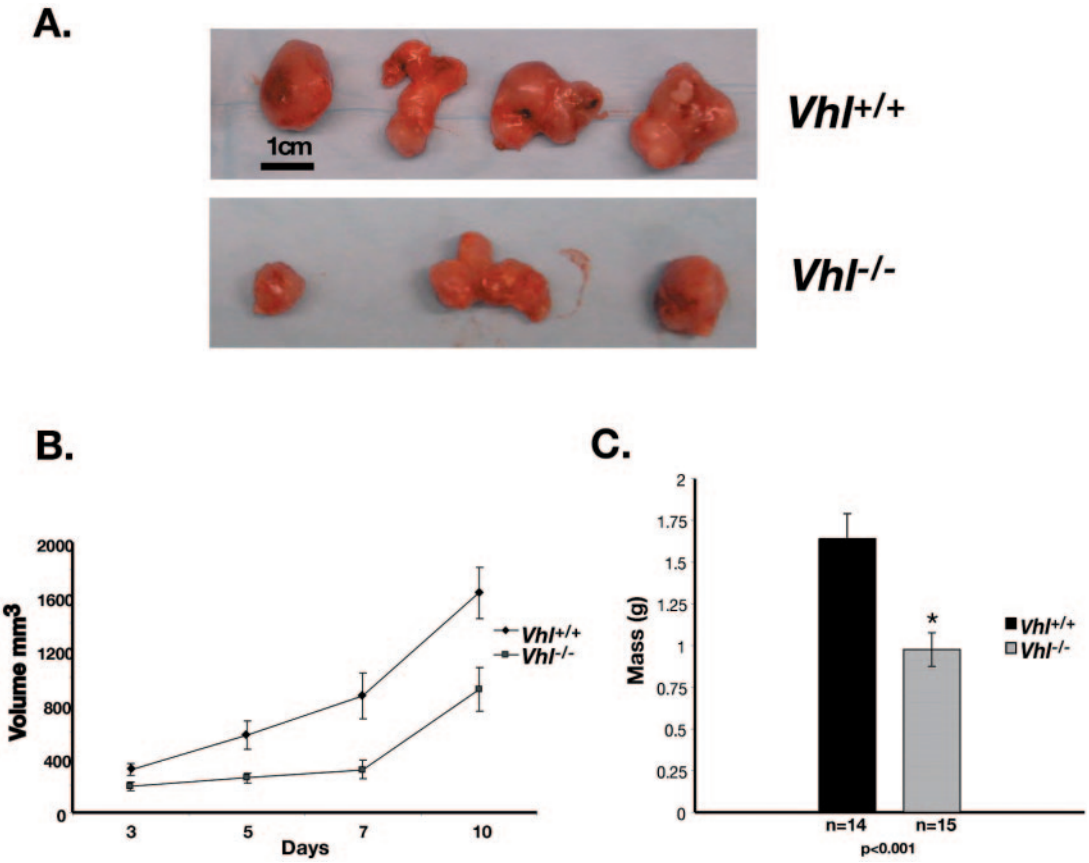

FIG. 2. Decreased growth of $Vhl^{-/-}$ fibrosarcomas. (A) Fibrosarcomas were formed by injecting MEFs subcutaneously into nude mice. $Vhl^{-/-}$ fibrosarcomas were smaller than controls. (B) Tumor growth was ascertained by tumor volume measurements over the course of 12 to 14 days. $Vhl^{-/-}$ fibrosarcomas grew significantly slower than controls. (C) The masses of $Vhl^{+/+}$ and $Vhl^{-/-}$ fibrosarcomas were measured after 12 to 14 days of growth. Student's *t* test revealed a statistically significant difference between tumor masses ($P < 0.001$).

percentage of $Vhl^{-/-}$ cells stained positive for Ki67 than for BrdU (42% versus 15.2%, respectively), implying that a majority of the mutant cells are in G_1 or G_2/M phase. The extent of apoptosis in fibrosarcomas was ascertained by TUNEL staining or immunohistochemistry to detect the apoptotic marker activated caspase-3. No significant differences were observed between $Vhl^{+/+}$ and $Vhl^{-/-}$ tumors in terms of the number of activated caspase-3^+ or $TUNEL^+$ cells (Fig. 4E to H). Necrotic regions were extensive in both tumor types, confounding analysis by morphometric software to quantify the number of apoptotic cells; therefore, tumor protein homogenates were analyzed for the expression of activated caspase-3. Recapitulating the results of the immunohistochemistry analysis, activated caspase-3 levels were not elevated and in fact slightly reduced in $Vhl^{-/-}$ fibrosarcomas when normalized to a loading control (Fig. 4K). Hence, the growth defects of *Vhl*-null teratomas and fibrosarcomas are attributed to aberrant cell cycle progression and not increased apoptosis.

***Vhl*$^{-/-}$ MEFs exhibit proliferation defects in vitro.** In addition to the activation of genes that promote cellular proliferation, hypoxia (through both HIF-dependent and -independent pathways) can also induce growth arrest (8, 11, 12). Given the reduction in the number of proliferating cells within $Vhl^{-/-}$ tumors, the in vitro cell cycle profile of $Vhl^{-/-}$ MEFs was analyzed. BrdU incorporation was analyzed in MEFs grown asynchronously in monolayer cultures under normoxic and hypoxic (0.5% O_2) conditions. Prolonged exposure to hypoxia reduced the percentage of cells in S phase by approximately 50% in wild-type MEF cultures, consistent with reports of hypoxia inducing a G_1 arrest in immortalized MEFs and primary B cells (11). Importantly, the percentage of cells in S phase in $Vhl^{-/-}$ cultures was markedly reduced compared to that of $Vhl^{+/+}$ MEFs under conditions of both normoxia and hypoxia (Fig. 5). As noted for $Vhl^{-/-}$ tumor cells, a greater proportion of $Vhl^{-/-}$ MEFs were in the G_2/M phase than the controls. Based on annexin V staining, apoptosis was not increased by a lack of pVHL or hypoxia (data not shown). The decreased proportion of $Vhl^{-/-}$ cells in S phase resulted in an approximately twofold increase in doubling time compared to that of $Vhl^{+/+}$ MEFs (24 h versus 15 h) (Fig. 6A). Continued incubation of $Vhl^{+/+}$ MEFs under hypoxia reduced cellular proliferation rates to levels similar to those of $Vhl^{-/-}$ MEFs. Furthermore, prolonged exposure of $Vhl^{-/-}$ cells to hypoxia had only a slight effect on proliferation rates (Fig. 6B and C). Therefore, the loss of pVHL mimics a constant hypoxic state and decreases cellular proliferation in MEFs.

Elevated expression of p21 and p27 in normoxic *Vhl*$^{-/-}$ MEF cultures. G_1 arrest mediated by hypoxia is reported to result from an induction of CKIs p21 and p27 (8, 11). The expression of CKIs and G_1/S cyclins was examined in an at-

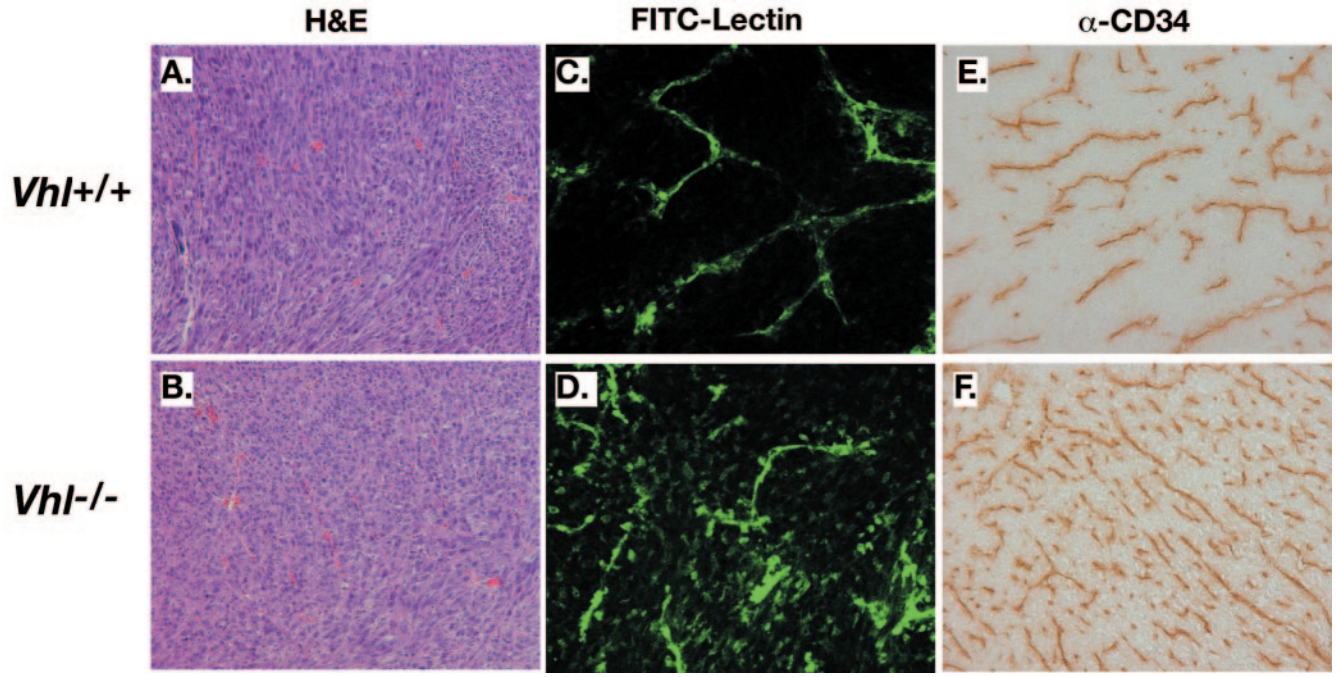

FIG. 3. Increased vascular permeability and vessel density in $Vhl^{-/-}$ fibrosarcomas. (A and B) Hematoxylin and eosin staining did not indicate any significant differences in histology between $Vhl^{+/+}$ and $Vhl^{-/-}$ fibrosarcomas. (C and D) Lectin perfusion of fibrosarcomas revealed highly organized vessel formation in $Vhl^{+/+}$ tumors, while $Vhl^{-/-}$ tumors demonstrated increased vascular permeability as noted by an increase in background fluorescence. (E and F) CD34 staining of fibrosarcomas. Note the increased vessel density in $Vhl^{-/-}$ fibrosarcomas. Final magnification, ×160.

tempt to explain the growth defect of $Vhl^{-/-}$ cells. Cell cycle synchronization by multiple methods, i.e., serum withdrawal and nocodazole treatment, could not be achieved in our immortalized, transformed MEF populations. Therefore, asynchronously cycling cells were assayed, and hypoxia (0.5% O_2) modestly induced the expression of p27 and p21 in $Vhl^{+/+}$ MEFs (Fig. 6D). Strikingly, both p27 and p21 protein levels were greatly elevated in $Vhl^{-/-}$ MEFs and not further increased by prolonged exposure to hypoxia (Fig. 6D, top panel). The induction of p21 and p27 was also observed in ES cells; two independent $Vhl^{-/-}$ ES cell lines displayed elevated levels of the CKIs, which were not further induced by hypoxia (Fig. 6D, bottom panel). In direct contrast, expression patterns of G_1/S cyclins (cyclin A, cyclin E, and cyclin D1) were unchanged by hypoxia in $Vhl^{+/+}$ and $Vhl^{-/-}$ MEFs. Furthermore, neither the expression of CDK2 (a G_1/S-phase cyclin-dependent kinase) nor its phosphorylation status was affected by hypoxia or pVHL absence (Fig. 6E). Our results demonstrate that a loss of pVHL leads to the dysregulation of p27 and p21 expression in both primary and transformed cells, profoundly affecting cellular proliferation rates.

CKIs inhibit G_1/S progression by binding to cyclin A-CDK2 and cyclin E-CDK2 complexes, thereby preventing the association and subsequent phosphorylation of substrates such as the retinoblastoma protein (pRB), a key regulatory event in the transition from G_1 to S phase. The elevated levels of p27 in $Vhl^{-/-}$ MEFs should therefore cause it to bind to cyclin A and cyclin E complexes, decreasing CDK2-associated kinase activity and promoting G_1/S arrest. Immunoprecipitation of cyclin A and cyclin E revealed an association of p27 with cyclin-CDK2 complexes under both normoxic and hypoxic conditions in $Vhl^{+/+}$ MEFs. The increased association of p27 to cyclin-CDK2 complexes in $Vhl^{-/-}$ MEFs was due to the higher levels of p27 expression in these cells compared with that of wild-type MEFs (Fig. 6F). However, in vitro kinase assays using extracts from asynchronously growing T Ag/H-Ras MEFs did not reveal a reduction in kinase activity associated with CDK2 or CDK4 (data not shown). These results may be explained by the fact that immortalized, transformed cells are defective in various cell cycle checkpoints, including the pRB and p53 pathways. Therefore, modest effects on CDK2 activity in asynchronously growing cells may not be apparent by in vitro kinase assays. However, proliferation rates and cell cycle profile data (Fig. 4, 5, and 6A to C) demonstrated that hypoxia can induce growth arrest in T Ag/H-Ras MEFs and that $Vhl^{-/-}$ MEFs exhibit defects in cellular proliferation in both in vitro and in vivo assays.

Elevated levels of p21 and p27 are not attributed to defects in protein degradation. Adhesion to the ECM can regulate cell cycle progression through G_1 phase by inducing the degradation of p21 and p27 (3). Attachment to fibronectin significantly affects the protein stabilization of p21. It has previously been shown that pVHL-null RCCs and primary MEFs are deficient in the assembly and deposition of fibronectin into the ECM (33). We therefore hypothesized that the growth defect of $Vhl^{-/-}$ MEFs may be due to a failure to deposit fibronectin, thereby preventing the proteolysis of p21 and p27. In this regard, $Vhl^{-/-}$ MEFs were analyzed for fibronectin deposition; an abundant fibronectin matrix was observed by immunofluorescence in $Vhl^{+/+}$ cells (Fig. 7A). Fibronectin deposition was

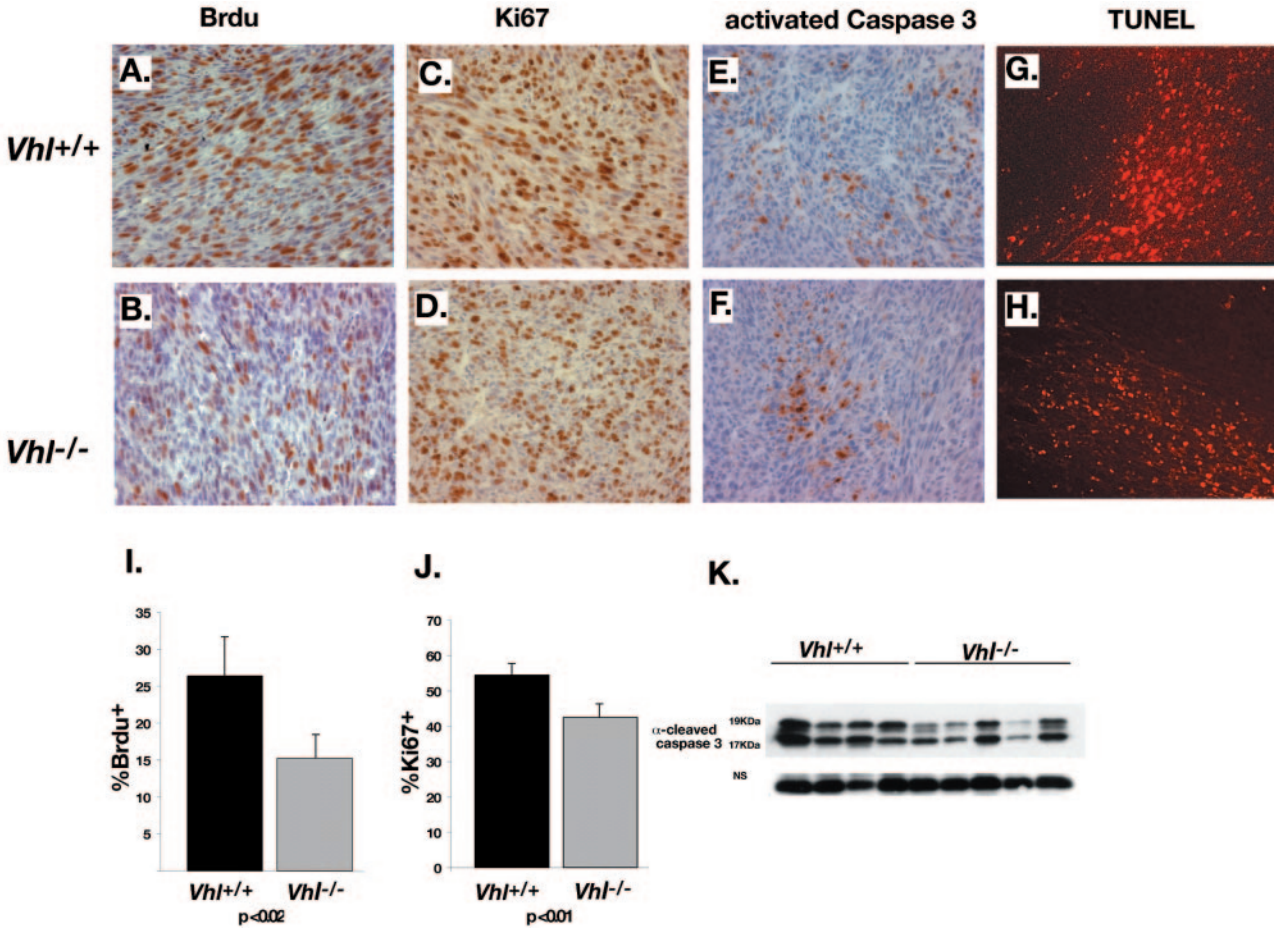

FIG. 4. The $Vhl^{-/-}$ growth defect is due to decreased cell proliferation. (A) BrdU incorporation into $Vhl^{+/+}$ fibrosarcomas highlights all cells within S phase. (B) Reduction in the number of $BrdU^{+}$ cells in $Vhl^{-/-}$ fibrosarcomas. (C) Expression of proliferation marker Ki67 indicates highly proliferating regions in $Vhl^{+/+}$ fibrosarcomas. (D) Proliferation as assessed by Ki67 staining also revealed a decrease in the number of actively cycling cells in $Vhl^{-/-}$ tumors. (E) Expression of apoptotic cell marker cleaved caspase-3 in $Vhl^{+/+}$ fibrosarcomas. (F) No differences in cleaved caspase-3 staining were apparent between $Vhl^{+/+}$ (E) and $Vhl^{-/-}$ fibrosarcomas. (G) Apoptosis as assessed by TUNEL staining in $Vhl^{+/+}$ tumors. (H) TUNEL staining did not reveal any differences in apoptosis between $Vhl^{+/+}$ (G) and $Vhl^{-/-}$ tumors. (I) Quantitation of $BrdU^{+}$ cells in $Vhl^{+/+}$ and $Vhl^{-/-}$ fibrosarcomas. A statistically significant reduction in the number of $BrdU^{+}$ cells in $Vhl^{-/-}$ fibrosarcomas was seen. (J) Quantitation of $Ki67^{+}$ cells in fibrosarcomas. The reduction in $Ki67^{+}$ cells in $Vhl^{-/-}$ MEFs was also found to be statistically significant. (K) Immunoblot to detect cleaved caspase-3 expression. No significant differences in apoptosis were apparent between $Vhl^{+/+}$ and $Vhl^{-/-}$ fibrosarcomas. A nonspecific (NS) band is shown as a loading control. Final magnification, ×160.

apparent in $Vhl^{-/-}$ MEFs, although the protein appeared to assemble into aberrant bundles not found in $Vhl^{+/+}$ cells (Fig. 7B). Growth upon fibronectin-coated plates resulted in a modest decrease in p21 and p27 (to a lesser degree) in $Vhl^{+/+}$ MEFs, while levels remained stable in cells grown on poly-L-lysine dishes. Protein levels of p21 and p27 remained high in $Vhl^{-/-}$ MEFs grown on either fibronectin or poly-L-lysine and were not reduced to wild-type levels after prolonged culture (Fig. 7E). Together, these results confirm that the dysregulation of p21 and p27 in $Vhl^{-/-}$ MEFs does not result from defects in ECM assembly.

One potential explanation for the elevated levels of these proteins is that p21 and p27 represent novel pVHL targets for ubiquitin-mediated degradation, even though the known E3 ubiquitin ligase responsible for p21 degradation contains Skp2 as the F-box protein. Protein turnover was therefore assessed by treatment with the translation inhibitor cycloheximide. Protein levels of p21 and p27, although more abundant in $Vhl^{-/-}$ MEFs, decreased at similar rates after cycloheximide treatment in $Vhl^{+/+}$ and $Vhl^{-/-}$ MEFs (Fig. 7F). Therefore, the elevated levels of p21 and p27 do not result from defects in protein proteolysis or pVHL-mediated degradation.

HIF antagonizes c-Myc transcriptional activity. Elevated p21 and p27 protein levels under hypoxia and in $Vhl^{-/-}$ MEFs could also result from increased mRNA transcription. To assess p21 and p27 mRNA levels, quantitative real-time PCR analysis was performed. Transcript levels of p21 and p27 were greatly elevated in $Vhl^{-/-}$ MEFs compared to those in $Vhl^{+/+}$ MEFs, over 100-fold and 5-fold higher, respectively (Fig. 8A). mRNA levels of direct HIF target genes *Vegf* and *Pgk* were also higher in $Vhl^{-/-}$ MEFs (10-fold and 2.6-fold, respectively) than in wild type-controls. Levels of c-Myc mRNA transcript were similar between wild-type and mutant cells. Hypoxia (0.5% O_2) induced the expression of all of the above genes, with the exception of c-Myc, between 2-fold and 10-fold over normoxic levels in $Vhl^{+/+}$ MEFs (Fig. 8A). In contrast, no

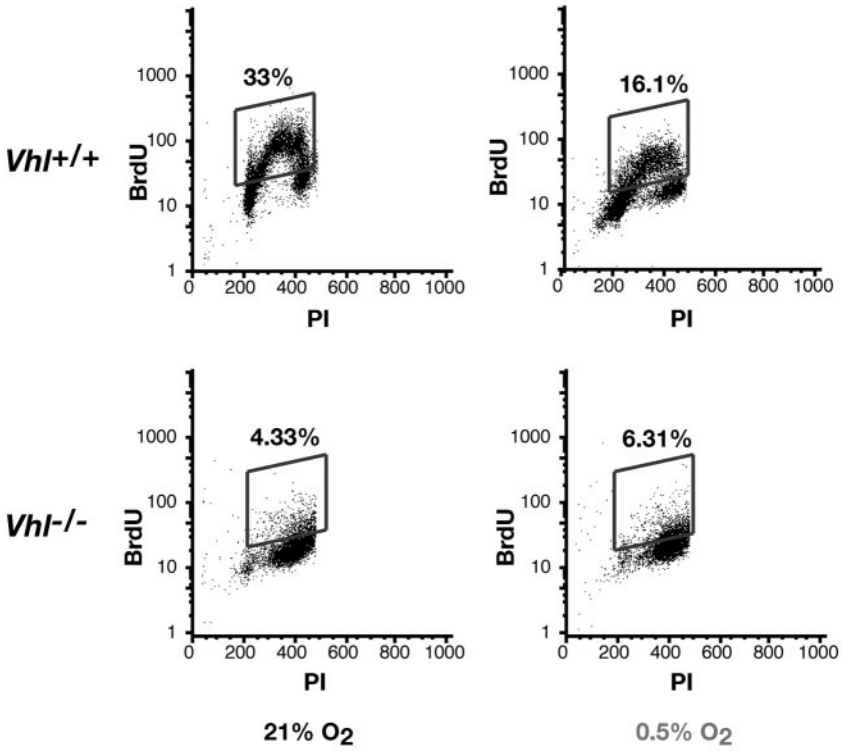

FIG. 5. Aberrant S-phase progression in $Vhl^{-/-}$ MEF cultures. BrdU incorporation was measured in $Vhl^{+/+}$ and $Vhl^{-/-}$ MEFs cultured under normoxic and hypoxic (0.5% O_2) conditions after 48 h. Hypoxia reduced the number of cells in S phase in wild-type cultures. Significantly fewer $Vhl^{-/-}$ MEFs were in S phase under normoxic conditions, and these numbers were not further reduced by hypoxic incubation.

hypoxic induction of these genes was seen in $Vhl^{-/-}$ MEFs. The slight hypoxic repression of gene transcription in $Vhl^{-/-}$ MEFs is attributed to HIF-independent hypoxic effects. While p21 and p27 mRNA levels are increased by hypoxia, their inductions have been reported to be significantly less than that noted for genes that contain HREs (11). Our work demonstrates that the hypoxic induction of at least p21 can exceed that of direct HIF targets, i.e., Vegf. Furthermore, these results suggest that dysregulation of transcription leads to elevated levels of p21 and p27 proteins.

The genes encoding p21 and p27 lack HREs normally found within the promoter or enhancer regions of O_2-regulated genes such as *Vegf* and *Epo*. Recent evidence indicates that HIF can induce p21 expression by preventing transcriptional repression by c-Myc. HIF has been shown to physically bind and interfere with c-Myc's interaction with cognate DNA binding sites, thereby antagonizing c-Myc transcriptional activity (23). c-Myc transactivation was therefore assessed in $Vhl^{+/+}$ and $Vhl^{-/-}$ MEFs using a c-Myc luciferase reporter assay (Fig. 8B). Of note, hypoxia repressed c-Myc reporter activity in $Vhl^{+/+}$ cells. Reporter activity was shown to be c-Myc responsive by cotransfection of a c-Myc expression plasmid. Furthermore, c-Myc reporter activity was markedly reduced in $Vhl^{-/-}$ cells under normoxic conditions, and no significant change occurred during hypoxia. The repression of c-Myc activity inversely correlated with the activation of HIF-mediated transcription under the same conditions (Fig. 8C). Reporter assays demonstrated elevated levels of HIF activity in hypoxic $Vhl^{+/+}$ cells which was repressed by cotransfection of pVHL. In contrast, HIF activity in $Vhl^{-/-}$ MEFs was greatly induced under normoxic conditions and not further elevated by hypoxia. HIF regulation was restored in $Vhl^{-/-}$ MEFs by cotransfection of pVHL. Our results are therefore consistent with recent data showing that stabilized HIF can inhibit c-Myc transcriptional repression, thus providing a potential mechanism for the induction of p21 and p27 under normoxia in $Vhl^{-/-}$ MEFs. Indeed, endogenous c-Myc was found to be associated with stabilized HIF-1α in $Vhl^{+/+}$ and $Vhl^{-/-}$ MEFs (data not shown).

To further demonstrate that the dysregulation of CKIs was dependent upon the antagonism of c-Myc transcriptional activity by HIF, gene silencing of c-Myc and HIF-1α by siRNA was performed in $Vhl^{+/+}$ and $Vhl^{-/-}$ MEFs. On average, c-Myc and HIF-1α protein levels were reduced by 70% by siRNA using transiently transfected double-stranded oligonucleotides (Fig. 9A). The reduction in c-Myc protein levels resulted in the elevation of p21 and p27 protein levels under normoxic conditions in $Vhl^{+/+}$ MEFs (Fig. 9B). However, treatment of $Vhl^{-/-}$ MEFs with c-Myc siRNA had no effect on p21 and p27 protein levels. This results from constitutively stabilized HIF-1α under normoxia within these cells, which prevents c-Myc-mediated repression of p21 and p27 expression. Conversely, elevated levels of p21 and p27 due to hypoxic exposure or loss of pVHL were decreased following HIF-1α siRNA treatment in $Vhl^{+/+}$ and $Vhl^{-/-}$ MEFs, respectively (Fig. 9B). The reduction in protein levels of c-Myc and HIF-1α also correlated with an inhibition of c-Myc-mediated repression of p21 and p27 transcription. Treatment with c-Myc siRNA elevated the mRNA levels of *p21* and *p27* by two- to

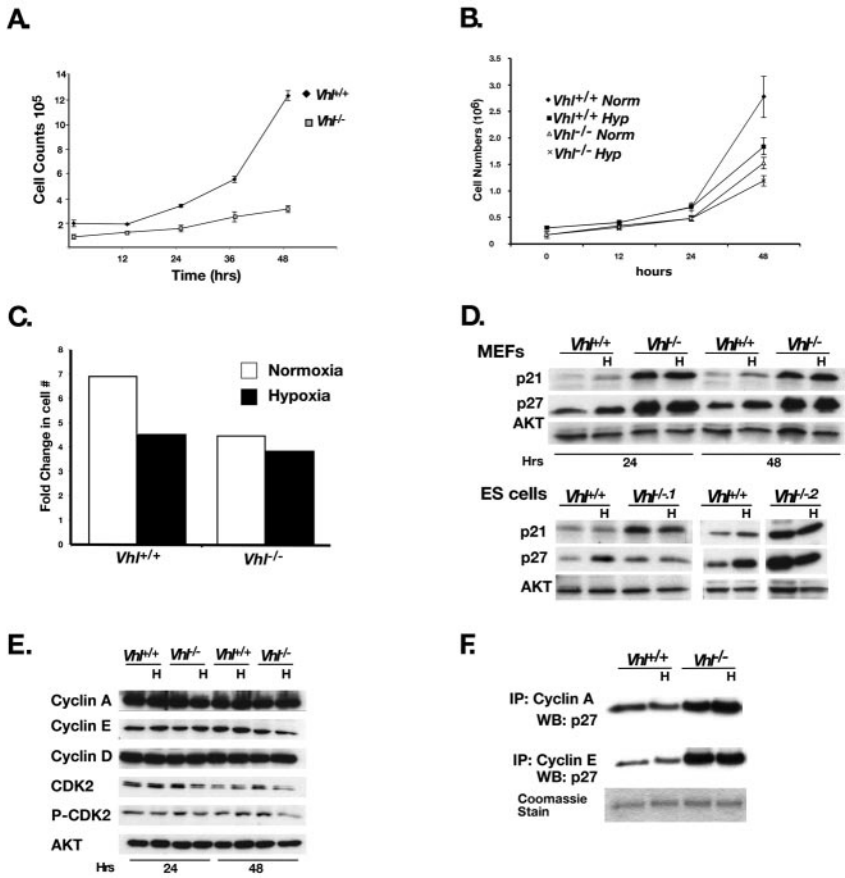

FIG. 6. $Vhl^{-/-}$ MEFs and ES cells exhibit elevated levels of p21 and p27. (A) Proliferation rate of $Vhl^{+/+}$ and $Vhl^{-/-}$ MEFs as assessed by cell counts. (B) Cell counts of $Vhl^{+/+}$ and $Vhl^{-/-}$ MEFs cultured under normoxia and hypoxia (0.5% O_2) for prolonged periods. (C) Graphical representation of proliferation rates of $Vhl^{+/+}$ and $Vhl^{-/-}$ MEFs under normoxia and hypoxia. (D) Immunoblots for p21 and p27 in $Vhl^{+/+}$ and $Vhl^{-/-}$ MEFs and ES cells under normoxia and hypoxia (0.5% O_2) for 48 h. $Vhl^{-/-.1}$ and $Vhl^{-/-.2}$ represent two independently derived $Vhl^{-/-}$ ES clones. Hypoxia induced the expression of p21 and p27 in $Vhl^{+/+}$ cells. Under normoxia, p21 and p27 levels were elevated in $Vhl^{-/-}$ cells and were not further induced by hypoxia. (E) Expression patterns of G_1 cyclins (cyclins A, E, and D), CDK2, and phosphorylated CDK2 remained unchanged under hypoxia or in the absence of pVHL. (F) Immunoprecipitations (IP) of cyclins E and A were immunoblotted for p27. The elevated levels of p27 in $Vhl^{-/-}$ MEFs remained associated with cyclin E and cyclin A complexes. Akt was used as a loading control.

threefold in normoxic $Vhl^{+/+}$ MEFs compared to control treated samples (Fig. 9C). Due to constitutively stabilized HIF-1α under normoxia, *p21* and *p27* mRNA levels were not enhanced in $Vhl^{-/-}$ MEFs treated with c-Myc siRNA. The slight reduction in the mRNA levels of p21 and p27 in $Vhl^{-/-}$ MEFs was not considered significant since protein levels were unchanged following c-Myc siRNA treatment. Exposure to 0.5% O_2 elevated p21 and p27 mRNA levels in $Vhl^{+/+}$ MEFs compared to normoxic control samples. Following HIF-1α siRNA treatment, the induction of p21 and p27 was reduced by two- to fivefold in $Vhl^{+/+}$ MEFs (Fig. 9C). Similarly, the expression levels of p21 and p27 were also markedly reduced in $Vhl^{-/-}$ MEFs treated with HIF-1α siRNA (Fig. 9C). The HIF target gene *Pgk* was used as a control for HIF transcriptional activation (data not shown). Furthermore, c-Myc siRNA-treated $Vhl^{+/+}$ MEFs exhibited reduced proliferation rates compared to control siRNA-treated cells (data not shown). The proliferation rate of $Vhl^{-/-}$ MEFs could be enhanced, compared to controls, by treatment with HIF-1α siRNA (data shown). Together, these results confirm that stabilized HIF-1α in $Vhl^{-/-}$ MEFs leads to the elevation of p21 and p27 by antagonizing c-Myc transcriptional activity.

DISCUSSION

Our study demonstrates that a loss of pVHL does not always correlate with increased tumor progression. Analysis of subcutaneous tumors formed with T Ag/H-Ras $Vhl^{-/-}$ MEFs revealed an inherent defect in cell growth. The slow growth and reduced mass of $Vhl^{-/-}$ tumors could not be attributed to a lack of vasculature; in fact, $Vhl^{-/-}$ tumors exhibited increased vessel density and permeability, consistent with the overexpression of HIF target genes such as *Vegf*. Furthermore, no differences in apoptosis were found between wild-type and $Vhl^{-/-}$ tumors. To elucidate the mechanism of pVHL effects on cellular proliferation, the cell cycle progression of $Vhl^{-/-}$ MEFs was examined. In culture, $Vhl^{-/-}$ MEFs exhibited a marked reduction in the number of cells in S phase, which resulted in a decrease in proliferation rate. Aberrant expression of cyclins, cyclin-dependent kinases, or cyclin-dependent kinase inhibi-

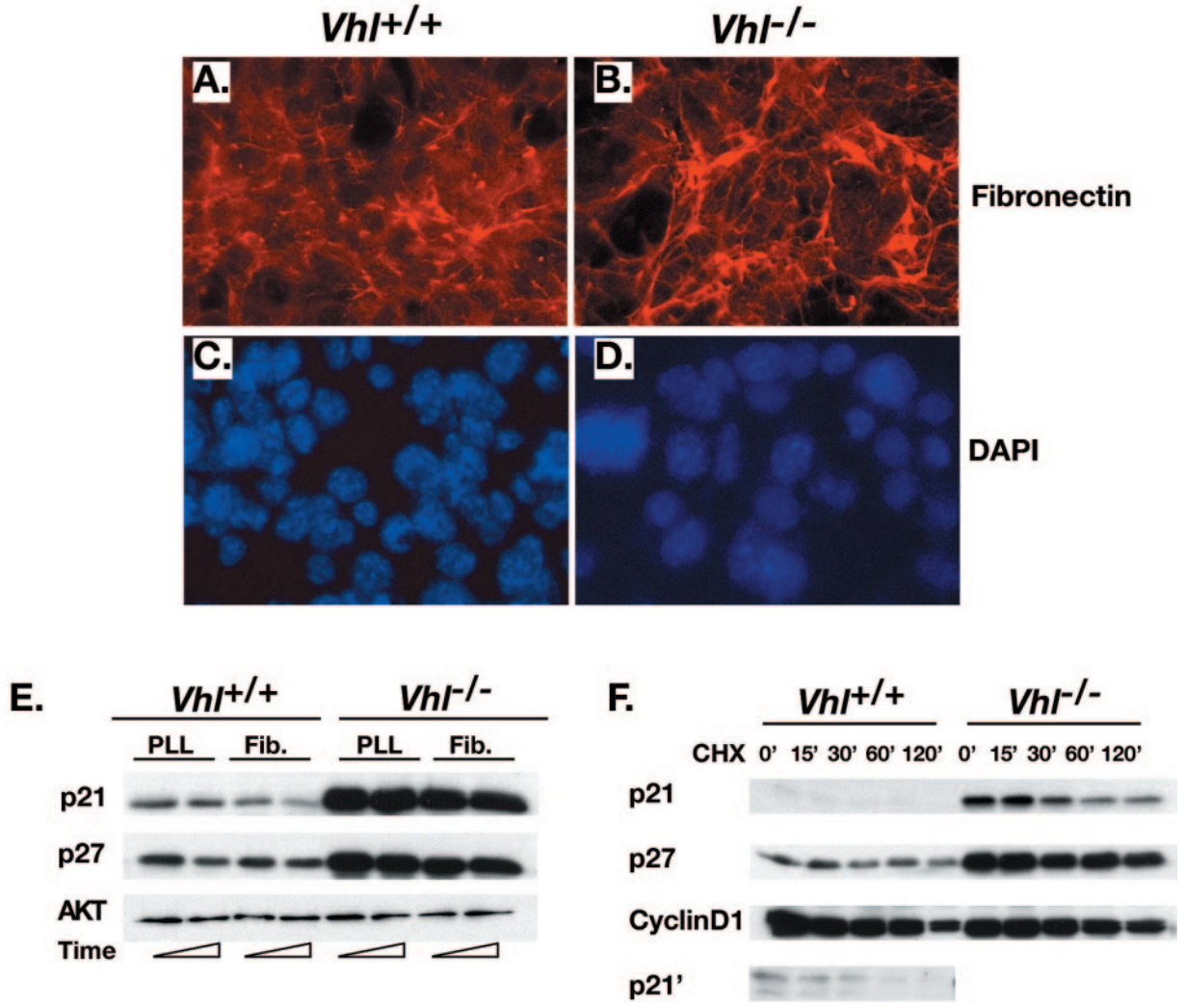

FIG. 7. $Vhl^{-/-}$ MEFs do not exhibit defects in the degradation of p21 and p27. (A and B) Immunofluorescence for fibronectin deposition. Fibronectin appeared to be uniformly deposited into the ECM in $Vhl^{+/+}$ MEFs. In contrast, fibronectin was assembled into aberrant bundles in $Vhl^{-/-}$ MEFs. (C and D) DAPI (4′,6′-diamidino-2-phenylindole) staining of nuclei in Fig. 6A and B. (E) Expression of p21 and p27 in whole-cell extracts of MEFs grown on fibronectin-coated (Fib.) or poly-L-lysine (PLL) dishes for 24 or 36 h. Prolonged culture of $Vhl^{+/+}$ MEFs on fibronectin decreased the expression of p21 and, to a lesser extent, p27. Culture of $Vhl^{-/-}$ MEFs on fibronectin did not reduce p21 or p27 expression to wild-type levels. (F) Expression of p21 and p27 in 20 μg of whole-cell extracts from MEFs treated with 200 μM cycloheximide (CHX) for the indicated times. Elevated levels of p21 and p27 were degraded in $Vhl^{-/-}$ MEFs at similar rates compared to wild-type cells. Cyclin D1 expression was reduced in both wild-type and mutant cells and therefore represents a control for cycloheximide treatment. p21′ is a prolonged exposure of 25 μg of $Vhl^{+/+}$ whole-cell extracts, which further demonstrated that the protein was degraded at similar rates in wild-type and mutant cells.

tors could lead to proliferation defects and was therefore examined. We found that p21 and p27 protein levels were highly elevated under normoxia and not further enhanced by hypoxia in both $Vhl^{-/-}$ MEFs and ES cells. Elevated levels of p21 and p27 were not mislocalized and remained associated with cyclin A-CDK2 and cyclin E-CDK2 complexes. Failure to assemble fibronectin into the ECM could also inhibit p21 and p27 proteolysis. Although fibronectin deposition by $Vhl^{-/-}$ MEFs was abnormal, adherence to fibronectin-coated dishes did not restore p21 or p27 degradation. Furthermore, protein turnover of p21 and p27 occurred at similar rates in $Vhl^{+/+}$ and $Vhl^{-/-}$ MEFs. We attributed elevated levels of p21 and p27 to HIF-mediated inhibition of c-Myc transcriptional activity (23). In the absence of hypoxic signaling, reduced c-Myc activity correlated with enhanced p21 and p27 transcription in $Vhl^{-/-}$ MEFs. The transcriptional repression of p21 and p27 by c-Myc could be restored in $Vhl^{-/-}$ MEFs by treatment with siRNA to HIF-1α, thereby reducing p21 and p27 mRNA and protein levels. Our results demonstrate that the loss of pVHL within primary ES cells and immortalized, transformed MEFs leads to cellular proliferation defects and induction of CKIs p21 and p27 through HIF-1α stabilization and antagonism of c-Myc transcriptional activity.

As stated previously, no inhibition of CDK2 kinase activity was observed in $Vhl^{-/-}$ MEFs, although elevated levels of p27 were associated with cyclin A/E-CDK2 complexes. This may be caused by the use of an asynchronous population (due to the inability to synchronize immortalized, transformed MEFs) or

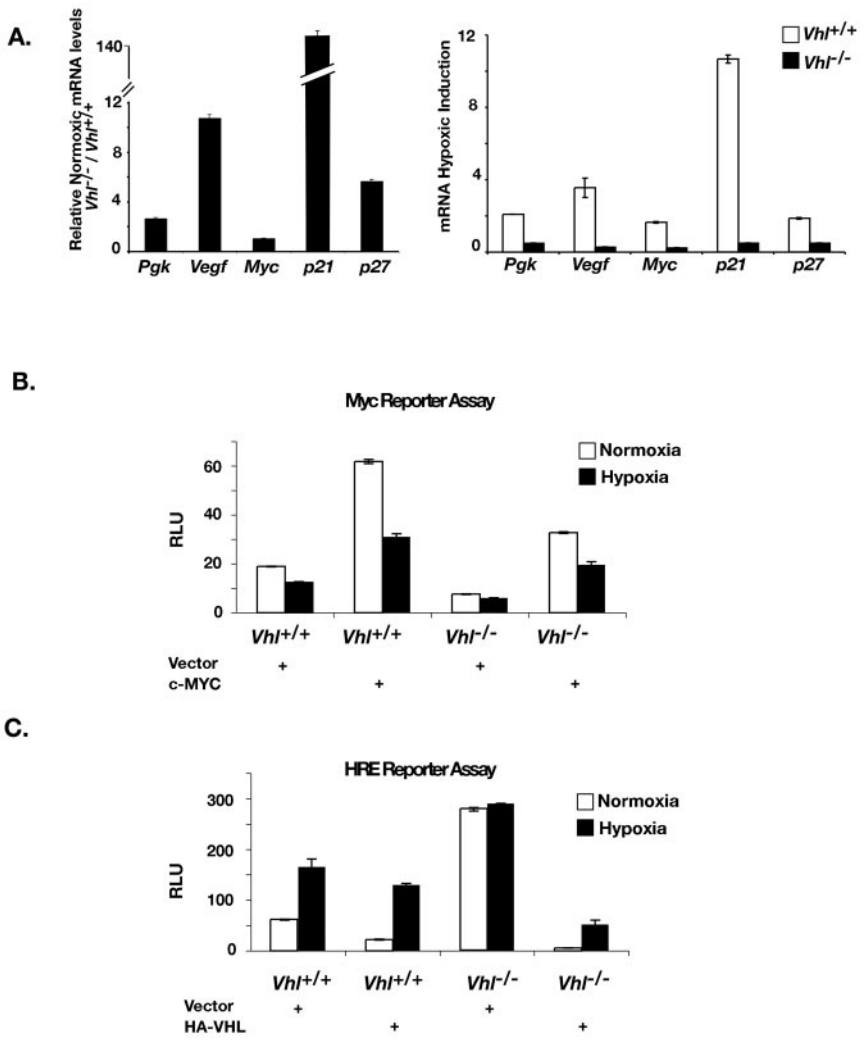

FIG. 8. HIF antagonizes c-Myc transcriptional activity. (A) Representative quantitative real-time PCR analysis for *Pgk*, *Vegf*, c-*Myc*, *p21*, and *p27* mRNA levels. Left, higher normoxic expression levels of *Pgk*, *Vegf*, *p21*, and *p27* in $Vhl^{-/-}$ MEFs compared to that of wild-type controls. Right, hypoxia greatly induced the expression of *Pgk*, *Vegf*, *p21*, and *p27* in $Vhl^{+/+}$ MEFs, while no induction of the genes was observed in $Vhl^{-/-}$ MEFs. Numbers indicate induction (*n*-fold) under hypoxia. Reactions were performed in triplicate and normalized to endogenous 18S RNA expression. (B) Myc transcriptional activity was reduced in $Vhl^{-/-}$ MEFs as determined by c-Myc reporter assays. Assays were performed in triplicate. (C) HIF transcriptional activity was elevated under conditions that repressed c-Myc activity. Hypoxia increased luciferase expression in $Vhl^{+/+}$ MEFs. However, luciferase expression was elevated in $Vhl^{-/-}$ MEFs under normoxia and not further induced by hypoxia. Regulation was restored by cotransfection of a plasmid encoding hemagglutinin-VHL. Cells were exposed to hypoxia as defined as 0.5% O_2 for 48 h.

by the limited sensitivity of the kinase assay. Furthermore, CDK2 kinase activity may be unaffected by increased p27 levels because of elevated cyclin D1 levels due to H-Ras activation. However, $Vhl^{-/-}$ MEFs clearly exhibit a cell cycle defect, even though CDK2 activity appeared to be unchanged. The number of cells in S phase was dramatically reduced in $Vhl^{-/-}$ MEF populations, although there was no accumulation of cells within G_1. Instead, the cell cycle profile of $Vhl^{-/-}$ MEFs indicated that the majority of the cells were in the G_2/M phase or undergoing endoreduplication. Elevated levels of p21 and p27 likely affect cyclin A/E-CDK2 complexes in $Vhl^{-/-}$ MEFs; however, these cells are unable to arrest in G_1 due to the inactivation of G_1/S checkpoints caused by large T Ag immortalization and H-Ras activation. This may promote endoreduplication or result in a failure to reenter the cycle. Alternatively, the arrest of $Vhl^{-/-}$ MEFs in the G_2/M phase may result from destabilization of microtubules in the absence of pVHL (14). Microtubule-destabilizing drugs such as nocodazole are frequently used to arrest cells in G_2/M without affecting CDK2 kinase activity.

Previous studies have shown that $VHL^{-/-}$ RCCs express elevated levels of cyclin D1, which leads to continued proliferation under a variety of growth-arresting conditions (2, 4). Furthermore, cyclin D1 has been suggested to be a pVHL-dependent hypoxia-inducible target gene based on microarray analysis in RCCs (40). Although reintroduction of pVHL restores the regulation of cyclin D1 in RCCs, this does not prove that a loss of pVHL is the direct cause of cyclin D1 dysregulation. Additionally, cyclin D1 expression is not regulated by pVHL in several nonrenal cell lines (4, 40). Furthermore, hyp-

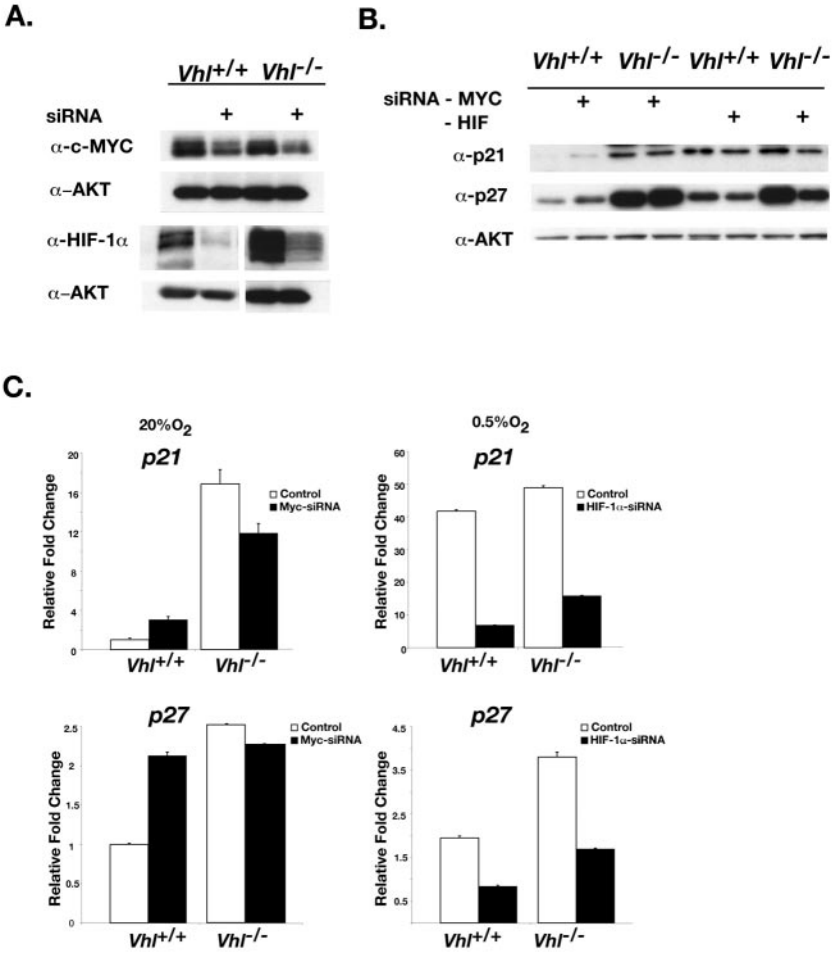

FIG. 9. Stabilized HIF-1α in $Vhl^{-/-}$ MEFs results in CKI elevation. (A) Treatment with c-Myc or HIF-1α siRNA reduced protein levels by 70% in $Vhl^{+/+}$ and $Vhl^{-/-}$ MEFs. (B) Immunoblot for p21 and p27 in siRNA-treated MEFs. Both p21 and p27 protein levels were induced in $Vhl^{+/+}$ MEFs treated with c-Myc siRNA, while no effect was seen in $Vhl^{-/-}$ MEFs. HIF-1α siRNA treatment resulted in a reduction in p21 and p27 protein levels in hypoxically treated $Vhl^{+/+}$ MEFs and $Vhl^{-/-}$ MEFs. Akt is shown as a loading control. (C) Representative quantitative real-time PCR for *p21* and *p27* mRNA levels. Numbers indicate the change (*n*-fold) in mRNA levels after siRNA treatment relative to control normoxia-treated $Vhl^{+/+}$ MEFs. c-Myc siRNA treatment induced the expression of p21 and p27 in $Vhl^{+/+}$ but not $Vhl^{-/-}$ MEFs, while HIF-1α siRNA treatment reduced the expression of p21 and p27 in both $Vhl^{+/+}$ and $Vhl^{-/-}$ MEFs. Assays were performed in triplicate and normalized to endogenous 18S RNA levels. Cells were exposed to hypoxia (0.5% O_2) for 48 h.

oxia results in the downregulation of cyclin D1 in Chinese hamster ovary (CHO), *Hif-1*$\alpha^{-/-}$, and *Hif-2*$\alpha^{-/-}$ ES cells (40). Of note, cyclin D1 levels remain unchanged by hypoxia in $Vhl^{+/+}$ and $Vhl^{-/-}$ MEFs in our studies. The selective hypoxic regulation of cyclin D1 in RCCs may contribute to the tissue specificity of VHL disease or perhaps is an indicator of additional tumorigenic pathways that are active within renal carcinomas.

Our results are consistent with a recent report showing that *Vhl* deletion or activation of the HIF pathway can lead to growth arrest in primary cells. Conditional inactivation of pVHL within cartilage results in severe dwarfism in otherwise viable mice due to a reduction in chondrocyte proliferation rates in bone growth plates (37). Conversely, the number of actively proliferating *Hif-1*$\alpha^{-/-}$ chondrocytes is increased at the periphery of the growth plate (38). These results confirm that pVHL may have a positive effect on cell cycle progression by antagonizing the HIF pathway in nonrenal cells. Analysis of early lesions within the kidneys of VHL patients revealed that the loss of pVHL in the proximal tubules does not confer a growth advantage. Multicellular focal lesions, indicating aberrant proliferation, were present in the distal tubules, while only single cellular focal lesions were found in the proximal tubules in which HIF activation was also seen (30). These results further substantiate our hypothesis that the loss of pVHL negatively affects cell growth in certain cell types, perhaps explaining the tissue specificity of VHL disease.

Whereas the induction of the HIF pathway appears to be essential to tumor vascular development, the initiating events of tumorigenesis may be mediated by specific activation of HIF-2α. pVHL-mediated tumorigenesis can be recapitulated in RCCs expressing a peptide derived from the ODD of HIF-1α but not a stabilized form of HIF-1α alone (31). pVHL-rescued RCCs infected to produce a constitutively stabilized HIF-2α fully retain their ability to form tumors in nude mice (22), while selective inactivation of HIF-2α suppresses tumor

growth as well as activation of glycolytic genes and angiogenic factors (21, 42). Expression of HIF-2α is O_2 regulated in ES cells but does not appear to contribute to the activation of glycolytic and angiogenic genes (C. J. Hu, and M. C. Simon, unpublished data). HIF-2α was not detected in our $Vhl^{+/+}$ and $Vhl^{-/-}$ MEFs, although HIF-2α has been reported to be constitutively stabilized and localized in the cytoplasm of other MEFs, preventing its ability to activate HIF-responsive genes (35). Our results suggest that the activation of HIF-1α can lead to growth arrest, which may provide a selective pressure during tumor progression to induce the expression of HIF-2α. Indeed, HIF-2α expression becomes more intense as renal cysts progress to overt clear-cell renal cell carcinomas in human VHL patients (30). Correlating HIF-2α expression and functional activity with the progression of other $Vhl^{-/-}$ tumors, i.e., pheochromocytomas and hemangioblastomas, would further support a role for HIF-2α as the primary target in *VHL*-mediated disease.

The ability of HIF to antagonize c-Myc transactivation represents a novel hypoxia-responsive pathway independent of HIF's DNA binding activity. Until recently, the induction of p21 and p27 was thought to be hypoxia dependent but HIF independent, due to the lack of HREs within their promoter regions. Koshiji et al. (23) have demonstrated that a constitutively stabilized and functional form of HIF-1α induces growth arrest via p21 induction in the absence of hypoxic signaling. Our work presents this model in an in vivo context where constitutive HIF-1α stabilization results in decreased tumor cell growth, further substantiating the importance of HIF–c-Myc interactions. Further experimentation will reveal whether this pathway is selectively lost during the progression of *VHL*-mediated tumorigenesis, perhaps through mutations in c-Myc itself. Indeed, amplification of c-Myc has been observed in renal clear-cell carcinomas (24). Analysis of the interplay between HIF-responsive genes and those antagonized through c-Myc inhibition will further elucidate the role of hypoxia and pVHL during tumorigenesis.

ACKNOWLEDGMENTS

We thank Q. C. Yu, Mercy Gohil, Michelle Mooney, Michele Hickey, Danielle Murphy, Jeff Tsai, Jay Hess, Thomas Yang, and Andrew Gladden for reagents and technical assistance.

This research was supported by National Institutes of Health grants HL63310 (M.C.S.) and 1F31HD (F.A.M.) and the Abramson Family Cancer Research Institute. M.C.S. is an investigator at the Howard Hughes Institute.

REFERENCES

1. **Arsham, A. M., D. R. Plas, C. B. Thompson, and M. C. Simon.** 2002. Phosphatidylinositol 3-kinase/Akt signaling is neither required for hypoxic stabilization of HIF-1 alpha nor sufficient for HIF-1-dependent target gene transcription. J. Biol. Chem. **277:**15162–15170.
2. **Baba, M., S. Hirai, H. Yamada-Okabe, K. Hamada, H. Tabuchi, K. Kobayashi, K. Kondo, M. Yoshida, A. Yamashita, T. Kishida, N. Nakaigawa, Y. Nagashima, Y. Kubota, M. Yao, and S. Ohno.** 2003. Loss of von Hippel-Lindau protein causes cell density dependent deregulation of CyclinD1 expression through hypoxia-inducible factor. Oncogene **22:**2728–2738.
3. **Bao, W., M. Thullberg, H. Zhang, A. Onischenko, and S. Strömblad.** 2002. Cell attachment to the extracellular matrix induces proteasomal degradation of $p21^{CIP1}$ via Cdc42/Rac1 signaling. Mol. Cell. Biol. **22:**4587–4597.
4. **Bindra, R. S., J. R. Vasselli, R. Stearman, W. M. Linehan, and R. D. Klausner.** 2002. VHL-mediated hypoxia regulation of cyclin D1 in renal carcinoma cells. Cancer Res. **62:**3014–3019.
5. **Blouw, B., H. Song, T. Tihan, J. Bosze, N. Ferrara, H. P. Gerber, R. S. Johnson, and G. Bergers.** 2003. The hypoxic response of tumors is dependent on their microenvironment. Cancer Cell **4:**133–146.
6. **Bruick, R. K.** 2000. Expression of the gene encoding the proapoptotic Nip3 protein is induced by hypoxia. Proc. Natl. Acad. Sci. USA **97:**9082–9087.
7. **Foster, K., A. Prowse, A. van den Berg, S. Fleming, M. M. Hulsbeek, P. A. Crossey, F. M. Richards, P. Cairns, N. A. Affara, M. A. Ferguson-Smith, et al.** 1994. Somatic mutations of the von Hippel-Lindau disease tumour suppressor gene in non-familial clear cell renal carcinoma. Hum. Mol. Genet. **3:**2169–2173.
8. **Gardner, L. B., Q. Li, M. S. Park, W. M. Flanagan, G. L. Semenza, and C. V. Dang.** 2001. Hypoxia inhibits G1/S transition through regulation of p27 expression. J. Biol. Chem. **276:**7919–7926.
9. **Gnarra, J. R., D. R. Duan, Y. Weng, J. S. Humphrey, D. Y. Chen, S. Lee, A. Pause, C. F. Dudley, F. Latif, I. Kuzmin, L. Schmidt, F. M. Duh, T. Stackhouse, F. Chen, T. Kishida, M. H. Wei, M. I. Lerman, B. Zbar, R. D. Klausner, and W. M. Linehan.** 1996. Molecular cloning of the von Hippel-Lindau tumor suppressor gene and its role in renal carcinoma. Biochim. Biophys. Acta **1242:**201–210.
10. **Gnarra, J. R., J. M. Ward, F. D. Porter, J. R. Wagner, D. E. Devor, A. Grinberg, M. R. Emmert-Buck, H. Westphal, R. D. Klausner, and W. M. Linehan.** 1997. Defective placental vasculogenesis causes embryonic lethality in VHL-deficient mice. Proc. Natl. Acad. Sci. USA **94:**9102–9107.
11. **Goda, N., H. E. Ryan, B. Khadivi, W. McNulty, R. C. Rickert, and R. S. Johnson.** 2003. Hypoxia-inducible factor 1α is essential for cell cycle arrest during hypoxia. Mol. Cell. Biol. **23:**359–369.
12. **Green, S. L., R. A. Freiberg, and A. J. Giaccia.** 2001. $p21^{Cip1}$ and $p27^{Kip1}$ regulate cell cycle reentry after hypoxic stress but are not necessary for hypoxia-induced arrest. Mol. Cell. Biol. **21:**1196–1206.
13. **Haase, V. H., J. N. Glickman, M. Socolovsky, and R. Jaenisch.** 2001. Vascular tumors in livers with targeted inactivation of the von Hippel-Lindau tumor suppressor. Proc. Natl. Acad. Sci. USA **98:**1583–1588.
14. **Hergovich, A., J. Lisztwan, R. Barry, P. Ballschmieter, and W. Krek.** 2003. Regulation of microtubule stability by the von Hippel-Lindau tumour suppressor protein pVHL. Nat. Cell Biol. **5:**64–70.
15. **Iliopoulos, O., A. Kibel, S. Gray, and W. G. Kaelin.** 1995. Tumour suppression by the human von Hippel-Lindau gene product. Nat. Med. **1:**822–826.
16. **Iliopoulos, O., A. P. Levy, C. Jiang, W. G. Kaelin, Jr., and M. A. Goldberg.** 1996. Negative regulation of hypoxia-inducible genes by the von Hippel-Lindau protein. Proc. Natl. Acad. Sci. USA **93:**10595–10599.
17. **Ivan, M., K. Kondo, H. Yang, W. Kim, J. Valiando, M. Ohh, A. Salic, J. M. Asara, W. S. Lane, and W. G. Kaelin, Jr.** 2001. HIFalpha targeted for VHL-mediated destruction by proline hydroxylation: implications for O2 sensing. Science **292:**464–468.
18. **Jaakkola, P., D. R. Mole, Y. M. Tian, M. I. Wilson, J. Gielbert, S. J. Gaskell, A. Kriegsheim, H. F. Hebestreit, M. Mukherji, C. J. Schofield, P. H. Maxwell, C. W. Pugh, and P. J. Ratcliffe.** 2001. Targeting of HIF-alpha to the von Hippel-Lindau ubiquitylation complex by O2-regulated prolyl hydroxylation. Science **292:**468–472.
19. **Johnson, R., B. Spiegelman, D. Hanahan, and R. Wisdom.** 1996. Cellular transformation and malignancy induced by ras require c-jun. Mol. Cell. Biol. **16:**4504–4511.
20. **Kamada, M., K. Suzuki, Y. Kato, H. Okuda, and T. Shuin.** 2001. von Hippel-Lindau protein promotes the assembly of actin and vinculin and inhibits cell motility. Cancer Res. **61:**4184–4189.
21. **Kondo, K., W. Y. Kim, M. Lechpammer, and W. G. Kaelin, Jr.** 2003. Inhibition of HIF2alpha is sufficient to suppress pVHL-defective tumor growth. PLoS Biol. **1:**E83.
22. **Kondo, K., J. Klco, E. Nakamura, M. Lechpammer, and W. G. Kaelin, Jr.** 2002. Inhibition of HIF is necessary for tumor suppression by the von Hippel-Lindau protein. Cancer Cell **1:**237–246.
23. **Koshiji, M., Y. Kageyama, E. A. Pete, I. Horikawa, J. C. Barrett, and L. E. Huang.** 2004. HIF-1alpha induces cell cycle arrest by functionally counteracting Myc. EMBO J. **23:**1949–1956.
24. **Kozma, L., I. Kiss, A. Nagy, S. Szakall, and I. Ember.** 1997. Investigation of c-myc and K-ras amplification in renal clear cell adenocarcinoma. Cancer Lett. **111:**127–131.
25. **Krieg, M., R. Haas, H. Brauch, T. Acker, I. Flamme, and K. H. Plate.** 2000. Up-regulation of hypoxia-inducible factors HIF-1alpha and HIF-2alpha under normoxic conditions in renal carcinoma cells by von Hippel-Lindau tumor suppressor gene loss of function. Oncogene **19:**5435–5443.
26. **Mack, F. A., W. K. Rathmell, A. M. Arsham, J. Gnarra, B. Keith, and M. C. Simon.** 2003. Loss of pVHL is sufficient to cause HIF dysregulation in primary cells but does not promote tumor growth. Cancer Cell **3:**75–88.
27. **Maher, E. R., and W. G. Kaelin, Jr.** 1997. von Hippel-Lindau disease. Medicine (Baltimore) **76:**381–391.
28. **Maltepe, E., B. Keith, A. M. Arsham, J. R. Brorson, and M. C. Simon.** 2000. The role of ARNT2 in tumor angiogenesis and the neural response to hypoxia. Biochem. Biophys. Res. Commun. **273:**231–238.
29. **Maltepe, E., J. V. Schmidt, D. Baunoch, C. A. Bradfield, and M. C. Simon.** 1997. Abnormal angiogenesis and responses to glucose and oxygen deprivation in mice lacking the protein ARNT. Nature **386:**403–407.
30. **Mandriota, S. J., K. J. Turner, D. R. Davies, P. G. Murray, N. V. Morgan, H. M. Sowter, C. C. Wykoff, E. R. Maher, A. L. Harris, P. J. Ratcliffe, and P. H. Maxwell.** 2002. HIF activation identifies early lesions in VHL kidneys:

evidence for site-specific tumor suppressor function in the nephron. Cancer Cell **1:**459–468.
31. **Maranchie, J. K., J. R. Vasselli, J. Riss, J. S. Bonifacino, W. M. Linehan, and R. D. Klausner.** 2002. The contribution of VHL substrate binding and HIF1-alpha to the phenotype of VHL loss in renal cell carcinoma. Cancer Cell **1:**247–255.
32. **Maxwell, P. H., M. S. Wiesener, G. W. Chang, S. C. Clifford, E. C. Vaux, M. E. Cockman, C. C. Wykoff, C. W. Pugh, E. R. Maher, and P. J. Ratcliffe.** 1999. The tumour suppressor protein VHL targets hypoxia-inducible factors for oxygen-dependent proteolysis. Nature **399:**271–275.
33. **Ohh, M., R. L. Yauch, K. M. Lonergan, J. M. Whaley, A. O. Stemmer-Rachamimov, D. N. Louis, B. J. Gavin, N. Kley, W. G. Kaelin, Jr., and O. Iliopoulos.** 1998. The von Hippel-Lindau tumor suppressor protein is required for proper assembly of an extracellular fibronectin matrix. Mol. Cell **1:**959–968.
34. **Okuda, H., K. Saitoh, S. Hirai, K. Iwai, Y. Takaki, M. Baba, N. Minato, S. Ohno, and T. Shuin.** 2001. The von Hippel-Lindau tumor suppressor protein mediates ubiquitination of activated atypical protein kinase C. J. Biol. Chem. **276:**43611–43617.
35. **Park, S. K., A. M. Dadak, V. H. Haase, L. Fontana, A. J. Giaccia, and R. S. Johnson.** 2003. Hypoxia-induced gene expression occurs solely through the action of hypoxia-inducible factor 1 α (HIF-1α): role of cytoplasmic trapping of HIF-2α. Mol. Cell. Biol. **23:**4959–4971.
36. **Pause, A., S. Lee, K. M. Lonergan, and R. D. Klausner.** 1998. The von Hippel-Lindau tumor suppressor gene is required for cell cycle exit upon serum withdrawal. Proc. Natl. Acad. Sci. USA **95:**993–998.
37. **Pfander, D., T. Kobayashi, M. C. Knight, E. Zelzer, D. A. Chan, B. R. Olsen, A. J. Giaccia, R. S. Johnson, V. H. Haase, and E. Schipani.** 2004. Deletion of Vhlh in chondrocytes reduces cell proliferation and increases matrix deposition during growth plate development. Development **131:**2497–2508.
38. **Schipani, E., H. E. Ryan, S. Didrickson, T. Kobayashi, M. Knight, and R. S. Johnson.** 2001. Hypoxia in cartilage: HIF-1alpha is essential for chondrocyte growth arrest and survival. Genes Dev. **15:**2865–2876.
39. **Sowter, H. M., P. J. Ratcliffe, P. Watson, A. H. Greenberg, and A. L. Harris.** 2001. HIF-1-dependent regulation of hypoxic induction of the cell death factors BNIP3 and NIX in human tumors. Cancer Res. **61:**6669–6673.
40. **Wykoff, C. C., C. Sotiriou, M. E. Cockman, P. J. Ratcliffe, P. Maxwell, E. Liu, and A. L. Harris.** 2004. Gene array of VHL mutation and hypoxia shows novel hypoxia-induced genes and that cyclin D1 is a VHL target gene. Br. J. Cancer **90:**1235–1243.
41. **Yu, F., S. B. White, Q. Zhao, and F. S. Lee.** 2001. HIF-1alpha binding to VHL is regulated by stimulus-sensitive proline hydroxylation. Proc. Natl. Acad. Sci. USA **98:**9630–9635.
42. **Zimmer, M., D. Doucette, N. Siddiqui, and O. Iliopoulos.** 2004. Inhibition of hypoxia-inducible factor is sufficient for growth suppression of VHL−/− tumors. Mol. Cancer Res. **2:**89–95.